scientific reports

Check for updates

OPEN

Dysfunctional crosstalk between macrophages and fibroblasts under LPS-infected and hyperglycemic environment in diabetic wounds

Shivam Sharma[1,2] & Anil Kishen[1,2,3]✉

Diabetic wounds, especially diabetic foot ulcers, present a major clinical challenge due to delayed healing and prolonged inflammation. Macrophage-fibroblast interactions are essential for wound repair, yet this crosstalk is disrupted in diabetic wounds due to hyperglycemia and bacterial infection. This study investigates the dysfunctional communication between macrophages and fibroblasts, focusing on autocrine, paracrine, and juxtacrine signaling in simulated diabetic environments. Using monoculture and co-culture models of THP-1-derived macrophages and primary human dermal fibroblasts, we simulated conditions of normal glucose, LPS-induced infection, high glucose (with AGEs), and combined high glucose (with AGEs) and LPS. Macrophages in hyperglycemic and LPS-infected environments exhibited a pro-inflammatory M1 phenotype with elevated expression of CD80, and STAT1 and increased production of IL-1β, TNF-α, and MMP9. Fibroblast migration was significantly impaired under high glucose conditions, particularly in paracrine model. Secretome profiling showed heightened pro-inflammatory cytokines and proteases, with reduced anti-inflammatory markers (IL-10 and VEGF-A) under hyperglycemic conditions. Paracrine signaling exacerbated the inflammatory response, while juxtacrine signaling showed more moderate effects, conducive to healing. These findings highlight the pathological macrophage-fibroblast crosstalk in diabetic wounds, particularly under hyperglycemic and LPS-infected conditions, offering insights for potential immunomodulatory therapies aimed at restoring effective signaling and improving wound healing outcomes.

Keywords Diabetic wounds, Chronic inflammation, Macrophage-fibroblast communication, Immuno-stromal synapse, Paracrine signaling, Juxtacrine signaling

Diabetes Mellitus (DM) is a chronic metabolic disorder characterized by elevated blood glucose levels due to defects in insulin secretion, action, or both[1]. As reported by the International Diabetes Foundation, approximately 537 million people were living with diabetes in 2021, and this number is projected to reach 783 million by 2045[2]. Its systemic nature is underscored by the array of physiological complications it engenders, impacting multiple organs[3]. One of the major complications of DM is Diabetic Foot Ulcers (DFUs), affecting 19–34% of diabetics in their entire lifetime[4]. These non-healing wounds are followed by gangrenous tissue formation in the majority of the cases leading to limb amputations. 85% of amputations in diabetic patients are due to foot ulceration[5,6]. Moreover, people with diabetes and DFUs are 2.5 times more likely to die as compared to patients without a foot injury[7]. Diabetic wounds pose a tremendous economic burden on healthcare. According to the reports, the annual expenditure on these chronic wounds exceeds $700 billion worldwide[8] while the World Health Organization (WHO) anticipates that diabetes will be the 7th leading cause of death by 2030[9]. Hence, diabetic wounds are a snowballing threat to public health and the economy.

The cutaneous wound healing process necessitates the activation and mobilization of diverse cell types, encompassing fibroblasts, keratinocytes, endothelial cells, and inflammatory cells[10–12]. After the injury, circulating monocytes are recruited at the wound site and differentiate into macrophages as part of the innate immune response during the early stages of wound healing[13]. Macrophages, functioning as immune cells, are the primary responders and provide organizational cues for other cell types by secreting a diverse repertoire of regulatory molecules (growth factors, cytokines, and chemokines) relevant to wound healing[14]. Fibroblasts,

[1]The Kishen Lab, Dental Research Institute, University of Toronto, Toronto, Canada. [2]Faculty of Dentistry, University of Toronto, 124 Edward Street, Toronto, ON M5G 1G6, Canada. [3]Department of Dentistry, Mount Sinai Hospital, Toronto, Canada. ✉email: anil.kishen@dentistry.utoronto.ca

acting as stromal cells in the dermis, are the primary effectors, where they function to restore the physical integrity of dermal connective tissue via wound closure through proliferation and production and remodeling of the extracellular matrix (ECM)[11,15,16]. Macrophages and fibroblasts communicate through paracrine and juxtacrine interactions leading to a healthy and timely wound repair[17]. The reciprocal interactions occurring between macrophages and fibroblasts at the injury site can influence each other's phenotype and functional behavior[18–22]. Macrophages exhibit distinct activation states: classically activated (M1) and alternatively activated (M2) macrophages[14]. M1 macrophages are pro-inflammatory and linked to tissue injury and inflammation, while M2 macrophages are associated with tissue repair and fibrosis[23]. Research has demonstrated that M2 macrophages can enhance the fibrogenic activities of dermal fibroblasts by facilitating cell proliferation and myofibroblastic differentiation[22]. M2 macrophages promote wound healing by secreting connective tissue growth factor, stimulating fibroblast proliferation and migration through the AKT, ERK1/2, and STAT3 signaling pathways[24]. In turn, dermal fibroblasts have been observed to promote angiogenesis and M2 polarization during the wound healing process[25]. This dynamic interplay is crucial for timely and effective wound repair.

The healing process in diabetic wounds is collectively stalled by ischemia, neuropathy, hypoxia, and inflammation at the wound site, all owing to the hyperglycemic environment[26–28]. This results in impaired migration and proliferation of fibroblasts and keratinocytes, impaired angiogenic response in endothelial cells and impaired macrophage behaviour[29]. Dysregulated polarization of macrophages causes prolonged and heightened inflammation[30,31]. This leads to a dysfunctional crosstalk between macrophages and fibroblasts contributing to impaired wound healing. In addition to that, bacterial infection and excessive secretion of proteases exacerbate the condition of these non-healing ulcers[32,33]. Consequently, the timely restoration of the anatomic integrity of the skin with analogous function is decelerated[34].

Macrophages and fibroblasts in the diabetic wounds communicate via soluble autocrine, paracrine and juxtacrine signals associated with direct cell-cell contact[35,36]. Despite the acknowledged importance of the interplay between macrophages and fibroblasts in facilitating wound healing, there remains a notable gap in our understanding concerning their dysfunctional interactions within an in vitro autocrine, paracrine, and juxtacrine framework under simulated diabetic wound conditions. The current investigation is the first in vitro study that aims to understand the dysfunctional crosstalk between the macrophages and fibroblasts in the 'immuno-stromal synapse' of diabetic wounds. We dissected the cell-cell interactions spatially as autocrine, paracrine, or juxtacrine under lipopolysaccharide (LPS)-induced infection and advanced glycated end products (AGEs) rich hyperglycemia, mimicking the diabetic wound microenvironment.

Understanding this dysfunctional crosstalk highlights the importance of co-culture consideration while developing in vitro diabetic wound models to study the mechanisms of diabetic wound healing. Addressing this altered interplay between macrophages and fibroblasts in the context of diabetes could provide valuable insights for developing a better immunomodulatory therapeutic strategy targeted to alter macrophage function to affect fibroblast behaviour towards enhanced healing targeted in diabetic patient populations.

Methods

Cell lines

THP-1 monocytes: Human acute monocytic leukemia cells (THP-1 monocytes, ATCC TIB-202; American Type Culture Collection, Rockville, MD) were cultured in complete RPMI 1640 (Gibco, Grand Island, NY) with 10% heat-inactivated fetal bovine serum (Sigma-Aldrich, St Louis, MO), 1% antibiotic/antimycotic (Gibco, Grand Island, NY), and 0.1% β-mercaptoethanol (Gibco, Grand Island, NY) at 37 °C in a humidified atmosphere supplemented with 5% CO_2. THP-1 cells (2.5×10^5 cells/mL) were differentiated to macrophages on exposure to 100 nmol/L phorbol 12-myristate-13-acetate (Sigma-Aldrich, St Louis, MO) for 24 h in cell-culture treated 10 cm petri dishes (Fisher Scientific, Hampton, NH). This was followed by an overnight resting period with fresh RPMI without phorbol 12-myristate-13-acetate. Differentiation of THP-1 monocytes to macrophages was confirmed by the presence of cellular adhesion. Cells within the 3rd and 5th passage were used for experiments. Macrophages were detached using 10mM EDTA (pH 7.4) (BioShop Canada Inc., Burlington, ON).

Primary human dermal fibroblasts (HDFs): HDFs were generously gifted by Dr. Boris Hinz's laboratory at the Faculty of Dentistry, University of Toronto. These cells were maintained in complete Dulbecco's Modified Eagle's Medium (D5796, Sigma-Aldrich) supplemented with 10% heat-inactivated fetal bovine serum (Sigma-Aldrich, St Louis, MO) and 1% antibiotic/antimycotic (Gibco, Grand Island, NY) in a 37 °C incubator with 5% CO_2 and a humidified atmosphere in T-75 flasks. 0.05% Trypsin with 0.53mM EDTA was used to sub-culture the cells.

In vitro cell cultures

Both the cell lines were used within the 3rd and 5th passages. Cells were seeded in 24-well tissue culture-treated polystyrene plates (Sarstedt AG & Co. KG, Nümbrecht, Germany) and cultured for a period of 48 h in serum-free DMEM for all the experiments. All the experiments were performed in triplicates. Five different monoculture and co-culture formats were established as follows (Fig. 1):

a. Macrophages monoculture: Macrophages were detached and seeded in 24 well plates. These were incubated for 24 h for re-attachment and then treated with four different media conditions: (i) Normal glucose (5mM), (ii) Normal glucose (5mM) with 1 μg/mL LPS[37], (iii) High glucose (25mM)[38] with 20 μg/mL AGEs[39,40] and (iv) High glucose (25mM) with 20 μg/mL AGEs and 1 μg/mL LPS referred to as NG, NGLPS, HG and HGLPS respectively in this article. 24 h post-treatment, macrophage conditioned media was collected, centrifuged at 10,000 x g for 10 min and stored at -80 °C for further analysis.
b. Fibroblasts monoculture: Fibroblasts cultured alone were treated with NG, NGLPS, HG and HGLPS culture conditions as detailed above in 24 well plates.

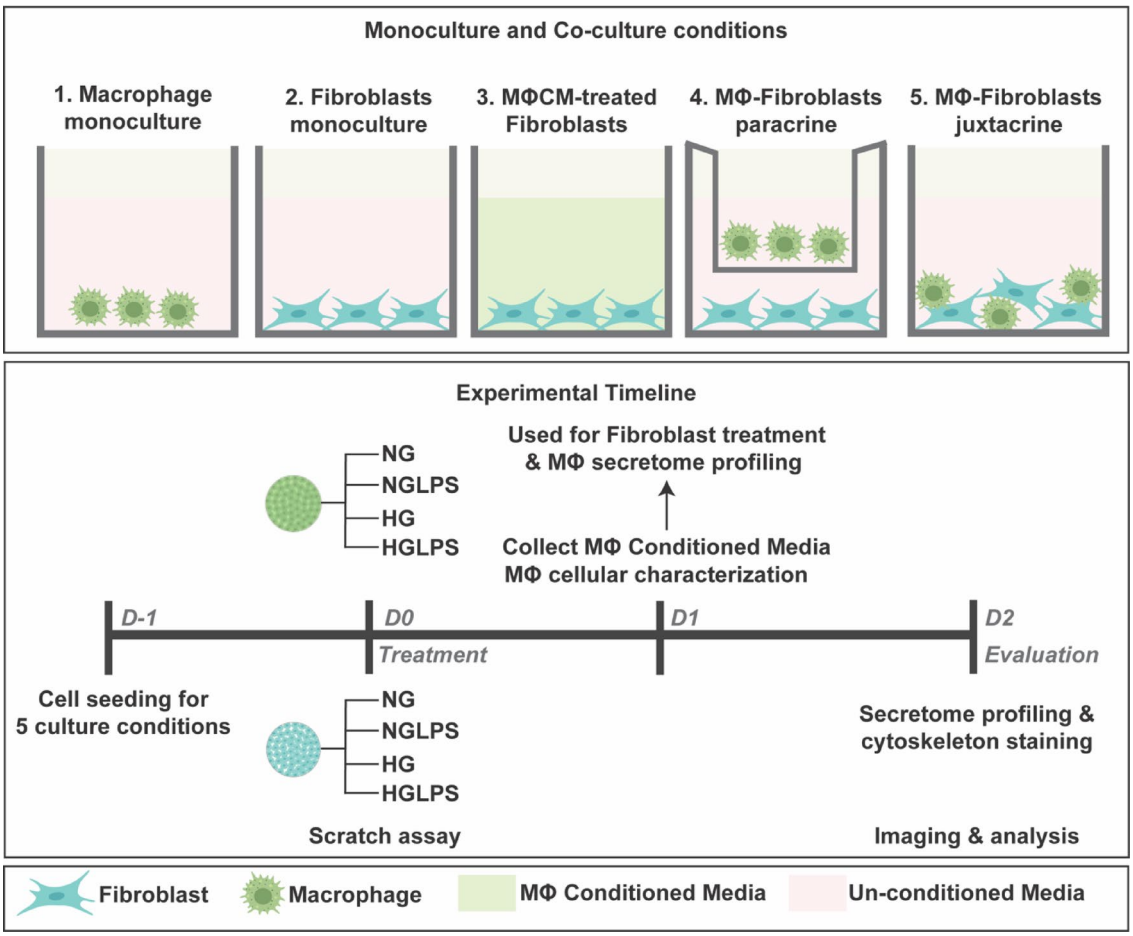

Fig. 1. Schematic showing five monoculture and co-culture conditions for macrophages and fibroblasts and the experimental timeline (NG: Normal glucose, NGLPS: Normal glucose with LPS, HG: High glucose with AGEs, HGLPS: High glucose with AGEs and LPS, MΦCM – Macrophage conditioned media).

c. Fibroblasts cultured with macrophage conditioned media: 24-hour conditioned media from macrophage monoculture (NG, NGLPS, HG and HGLPS) was thawed at 37 °C and added on fibroblasts cultured in 24 well plates.
d. Macrophages-fibroblasts paracrine culture: 1:1 ratio of macrophages to fibroblasts were co-cultured as fibroblasts at the bottom of the well and macrophages in the trans well inserts (Corning Inc., Corning, NY) and treated with similar NG, NGLPS HG and HGLPS media conditions.
e. Macrophages-fibroblasts juxtacrine culture: Similar 1:1 ratio of macrophages and fibroblasts were mixed for co-culture in a 24 well plate and treated with NG, NGLPS, HG and HGLPS media conditions.

LPS from *Pseudomonas Aeruginosa* 10 (Sigma-Aldrich, St Louis, MO) and AGE-BSA (Abcam, Cambridge, UK) were used for preparing different media for treatment of cells as described above.

Macrophage cellular characterization

After treatment with NG, NGLPS, HG, HGLPS for 24 h, macrophages were stained for the cluster of differentiation (CD) markers- CD80, CD206, and CD68 using anti-CD80-AF594 (Cedarlane, Burlington, ON), anti-CD206-AF488 (BioLegend, San Diego, CA) and anti-CD68-AF647 (BioLegend, San Diego, CA) antibodies respectively and signal transducer and activator of transcription (STAT) markers- STAT1, STAT3, and STAT6 using anti-STAT1-AF594 (BioLegend, San Diego, CA), anti-STAT3-AF647 (BioLegend, San Diego, CA) and anti-STAT6-AF594 (Santa Cruz Biotechnology, Dallas, TX) antibodies according to the standard staining protocol using optimal dilution of the antibody. Imaging was done using Nikon Epifluorescence microscope (Nikon Eclipse Ti2-E) at 10X objective magnification at appropriate channels. Images were quantified using IMARIS 10.0.1 software. The intensity sum and area sum were calculated after thresholding the cells against the background. The intensity sum was standardized with the area sum to be plotted for comparisons of different conditions.

Scratch migration assay

Fibroblasts were seeded in each well at a density of 10^5 cells for monoculture and macrophage conditioned media treatment. A total of 10^5 macrophages and 10^5 fibroblasts were co-cultured for paracrine and juxtacrine settings

as detailed above. A cellular monolayer was obtained after 24-hour incubation in CO_2 incubator at 37 °C. Using a 200µL micropipette tip a cruciate-shaped scratch was created to have a cell-free zone on the cellular monolayer. The cells were gently washed with PBS (Gibco, Thermo Fisher Scientific, Waltham, MA) to remove any debris. Treatment was done with serum-free NG, NGLPS, HG and HGLPS media for 48 h. Brightfield imaging was performed immediately after the scratch was created (0-hour) and at the 48-hour time point. Imaging was performed using a Nikon Epifluorescence microscope (Nikon Eclipse Ti2-E, Nikon Instruments, Tokyo) at 4X objective magnification. The scratch area was quantified using wound healing size tool in FIJI software (Fiji is Just ImageJ version 2.16.0/1.54p)[41] and the % area coverage was calculated using the Eq. (1) and standardized to the control (NG) values.

$$\% \text{ Area coverage} = \frac{\text{Area } (0) - \text{ Area } (t)}{\text{Area } (0)} \text{ X } 100 \quad (1)$$

In the Eq. (1), Area (0) refers to the area of the scratch at time point 0-hour and Area (t) refers to the area of the scratch at time point t.

Secretome profiling

All five macrophages and fibroblasts monoculture and co-culture settings were established as detailed above. These cultures were treated with NG, NGLPS, HG and HGLPS DMEM for 48 h. This cell culture media was collected, centrifuged at 10,000 x g for 10 min and analyzed for secretome analysis using immunology multiplex assay according to the manufacturer's instructions. The cytokines IL-1β, TNF-α, IL-6, IL-1RA, IL-10; chemokines IL-8, MCP-1 (CCL2), MIP1-α (CCL3), MIP1-β (CCL4), RANTES (CCL5); and growth factor VEGF-A were analyzed using MILLIPLEX® Human Cytokine/Chemokine/Growth Factor Panel A (#HCYTA-60 K, Millipore Sigma), TGF-β using MILLIPLEX® TGFβ1 Magnetic Bead Single Plex Kit (#TGFBMAG-64 K, Millipore Sigma), MMP9 using MILLIPLEX® Human MMP Magnetic Bead Panel 2 kit (#HMMP2MAG-55 K, Millipore Sigma), and TIMP1 using MILLIPLEX® Human TIMP Magnetic Bead Panel 2 kit (#HTMP2MAG-54 K, Millipore Sigma) were quantified. DMEM alone was used as a control for all the molecules. The levels of these molecules were compared with respect to NG as their baseline values.

Cell cytoskeleton staining

All five culture settings of macrophages and fibroblasts monoculture and co-cultures were established as detailed above. A total of 10^4 fibroblasts and 10^4 macrophages were seeded for monoculture, and a 1:1 ratio of macrophages to fibroblasts were seeded for co-culture conditions. The macrophage conditioned media were diluted with fresh DMEM at a similar ratio. After 48 h of treatment with NG, NGLPS, HG and HGLPS media, the cells were stained for vimentin using anti-vimentin-AF488 antibody (Santa Cruz Biotechnology, Dallas, TX) and actin using phalloidin-TRITC antibody according to the standard staining protocol and optimal dilution of the antibody. Imaging was performed using a Nikon Epifluorescence microscope (Nikon Eclipse Ti2-E, Nikon Instruments, Tokyo) at 10X objective magnification on appropriate fluorescence channels. Images were analyzed using IMARIS 10.0.1 software. Intensity sum and area sum were calculated after thresholding the cells against the background. The intensity sum was standardized with the area sum to be plotted for comparisons of different conditions.

Statistical analysis

All the experiments were performed in triplicate, and the data obtained are presented as the mean ± standard error of the mean. GraphPad Prism 10.1.1 (GraphPad, La Jolla, CA) was used to statistically evaluate the data. Statistical differences between more than two groups were analyzed using ordinary one-way ANOVA (analysis of variance) with the post-hoc Tukey test. A $P<0.05$ (95% confidence interval) was considered to indicate statistical significance.

Results

Macrophage polarization state

Cells were stained positive for CD80 and CD68 whereas CD206 was not expressed under any of the conditions (Fig. 2a). CD80 expression was higher compared to CD68 as noted based on the quantified intensities for all the groups (Fig. 2b). Both the CD80 and CD68 expressions were almost similar after treatment with high glucose and/or LPS (Fig. 2b). STAT marker staining revealed that STAT1 expression was significantly higher in high glucose with and without LPS groups compared to normal glucose control group ($P<0.05$) (Fig. 2c-f). The presence of LPS slightly increased that expression in their respective glucose concentrations group although not significantly different. STAT3 expression was significantly lower in the cells treated with the combination of high glucose and LPS ($P<0.05$) (Fig. 2c-f). On the other hand, STAT6 expression was lower in the high glucose environment compared to normal glucose environment (Fig. 2d-f).

Differential migration pattern of fibroblasts

Fibroblasts in monoculture showed enhanced migration after the addition of LPS to the normal glucose media group. However, high glucose combined with LPS significantly reduced the area coverage to 50% ($P<0.05$) (Fig. 3a). When fibroblasts were treated with conditioned media from macrophages, the healing pattern showed significant reduction in migration under a hyperglycemic environment with or without LPS both ($P<0.05$) (Fig. 3b). When co-cultured with macrophages in a dynamic paracrine system, fibroblasts exhibited a similar pattern of hyperglycemic-induced lower migration, although with a relatively lower percentage of 50% area coverage (Fig. 3c). In contrast, fibroblasts in direct co-culture with macrophages (juxtacrine) did not exhibit

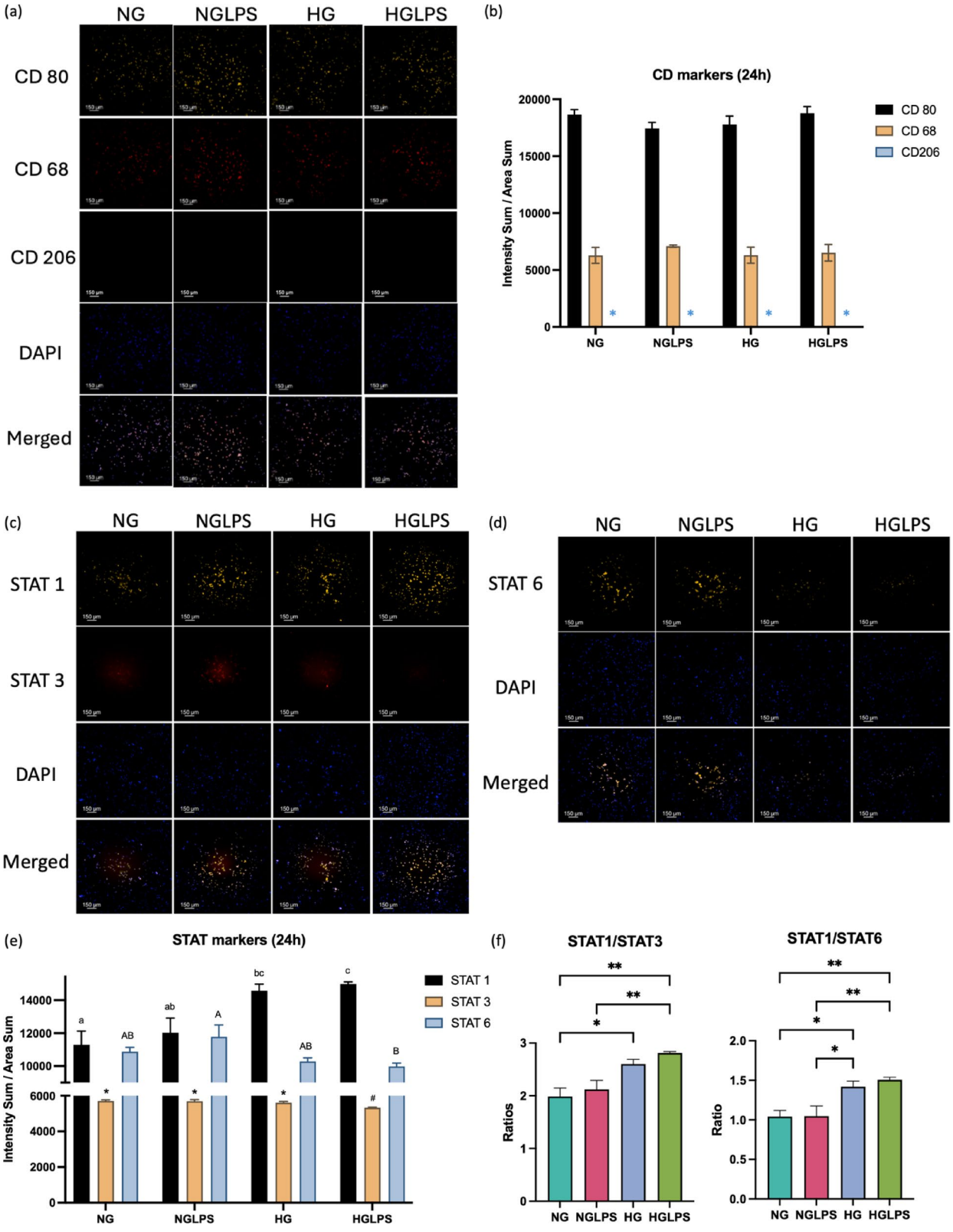

Fig. 2. Macrophage cellular characterization by CD and STAT markers staining and quantification. (* indicates that CD 206 value in graph b is zero).

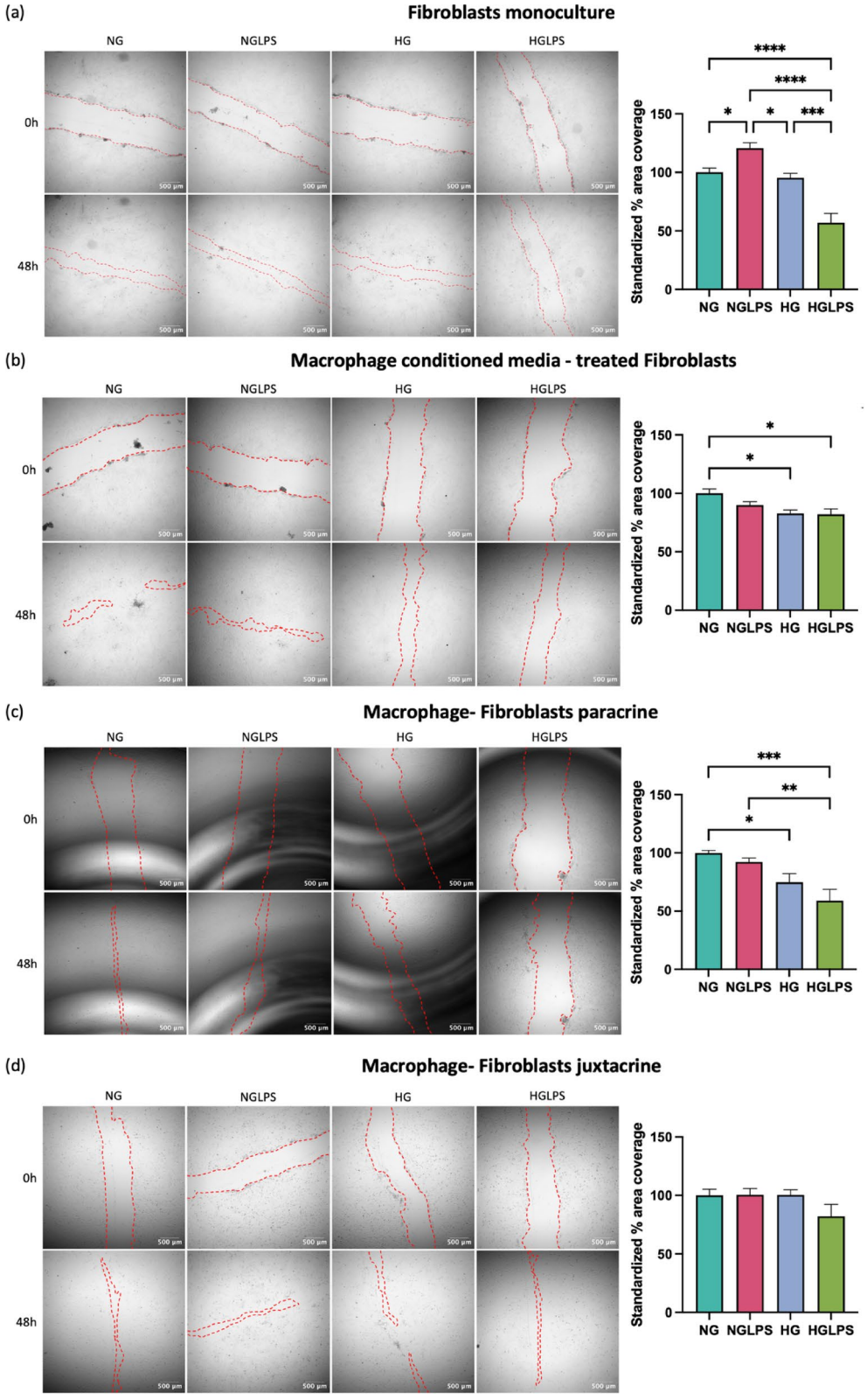

Fig. 3. In vitro scratch migration assay for fibroblasts in different monoculture and co-culture formats.

similar migration behavior (Fig. 3d). The high glucose with LPS group exhibited decreased migration (80%), but this difference was not significant.

Secretome profiles

Macrophages monoculture

The addition of LPS to normal glucose media could significantly increase the expression of the pro-inflammatory cytokines IL-1β, TNF-α, and IL-6; reduce the levels of the anti-inflammatory cytokine IL-1RA; VEGF-A; and increase the production of chemokines (IL-8, MCP-1, MIP1-α, MIP1-β, and RANTES) ($P<0.05$) (Fig. 4). In addition, MMP9/TIMP1 ratio was also significantly greater in the NGLPS group ($P<0.05$) (Fig. 4). The high glucose treatment group significantly reduced the levels of the anti-inflammatory cytokine IL-1RA; and chemokines IL-8, MCP-1 and RANTES. The MMP9/TIMP1 ratio was also significantly higher in the presence of high glucose ($P<0.05$) (Fig. 4). However, the IL-10 levels were significantly lower in the HG group compared to NGLPS ($P<0.05$) (Fig. 4). HGLPS showed higher production of the pro-inflammatory cytokines IL-1β, TNF-α, and IL-6; MMP9/TIMP1 ratio; and chemokines IL-8, MCP-1, MIP1-α, MIP1-β, and RANTES while almost similar levels of IL-1RA to those at the baseline (NG) (Fig. 4).

Fibroblasts monoculture

Molecules such as TNF-α, IL-6, IL-1RA, and IL-10 did not show any differential secretions, and IL-1β, MMP9, MIP1-α, and MIP1-β were not secreted by the fibroblasts alone in any of the groups (Figs. 5 and 6). LPS treatment of fibroblasts also did not significantly change the levels of TGF-β, VEGF-A, RANTES and IL-8 (Figs. 5 and 6). However, MCP-1 production was significantly increased in the LPS-treated cells ($P<0.05$) (Fig. 6c). HG media could increase the levels of TGF-β, VEGF-A, and the chemokines IL-8 and RANTES (Figs. 5f and 6a, b and f). HGLPS group showed increased production of VEGF-A, and the chemokines (IL-8, RANTES) (Fig. 6a, b, f). Interestingly, RANTES and MCP-1 levels in the HGLPS group were lower than those in the without LPS (HG) group (Fig. 6c, f).

Fibroblasts treated with macrophage conditioned media

When fibroblasts were treated with macrophage conditioned media, no significant differences were observed in the levels of IL-1β, IL-6, IL-10, and IL-8 levels among all the groups (Figs. 5 and 6). The LPS-treated group, NGLPS showed that the pro-inflammatory cytokine TNF-α; chemokines MCP-1, RANTES, MIP1-α and MIP1-

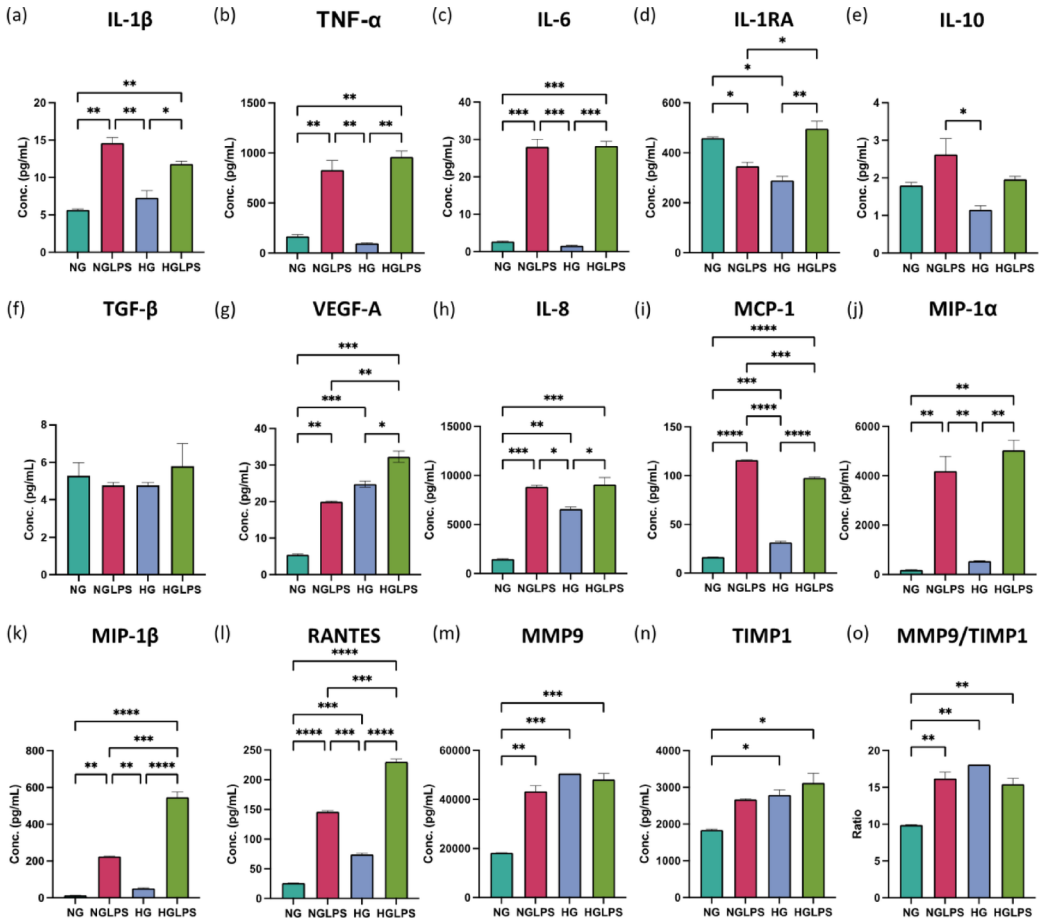

Fig. 4. Secretome profiling of the macrophage monoculture after 24 h of treatment.

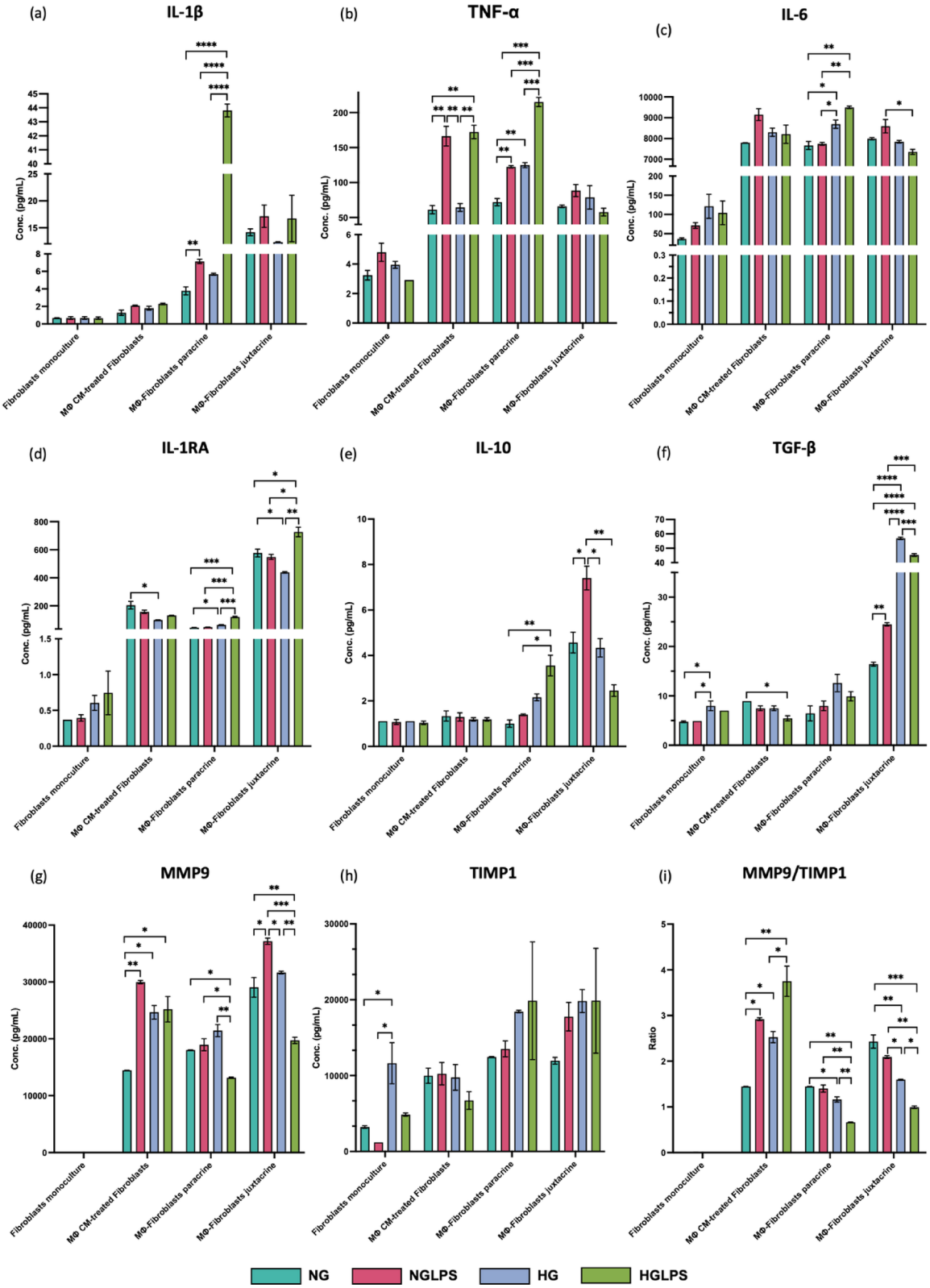

Fig. 5. Secretome profiling of fibroblasts under different monoculture and co-culture conditions showing the levels of cytokines IL-1β, TNF-α, IL-6, IL-1RA, IL-10, TGF-β; MMP9; TIMP1; and MMP9/TIMP1 ratio.

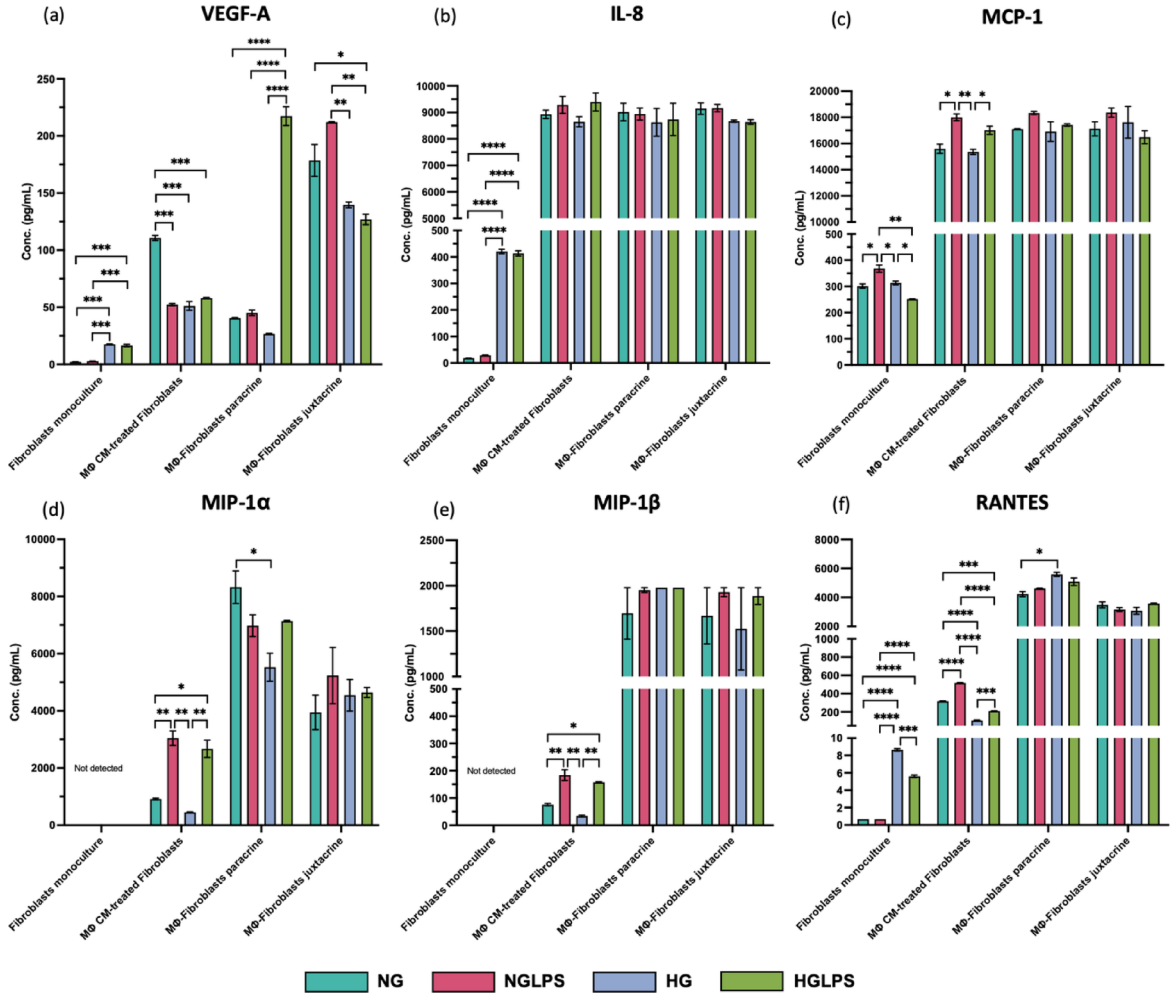

Fig. 6. Secretome profiling of fibroblasts under different monoculture and co-culture conditions showing the levels of chemokines IL-8, MCP-1, MIP1-α, MIP1-β, RANTES; and VEGF-A.

β; and MMP9/TIMP1 ratio were significantly increased; VEGF-A was significantly decreased while the anti-inflammatory cytokines IL-1RA and TGF-β were not affected ($P<0.05$) (Figs. 5 and 6). High glucose media conditions, in this case significantly increased the MMP9/TIMP ratio, decreased the anti-inflammatory cytokine IL-1RA; VEGF-A; chemokine RANTES while molecules MIP1-α, MIP1-β, MCP-1 and TGF-β were not affected ($P<0.05$) (Figs. 5 and 6). The addition of LPS to high glucose media (HGLPS) significantly increased the pro-inflammatory cytokine TNF-α; chemokines MIP1-α, MIP1-β; and MMP9/TIMP1 ratio ($P<0.05$) (Figs. 5 and 6). Moreover, it significantly decreased the anti-inflammatory cytokine TGF-β; VEGF-A; and chemokine RANTES ($P<0.05$) (Figs. 5 and 6). However, the levels of IL-1RA and MCP-1 were not changed under these conditions.

Macrophages-fibroblasts paracrine co-culture

When macrophages and fibroblasts were cultured in a continuous paracrine interaction setting, the anti-inflammatory cytokine TGF-β and chemokines IL-8, MCP-1, and MIP1-β were not affected in any of the groups (Figs. 5f and 6b, c and e). However, the addition of LPS to normal glucose media significantly increased the levels of pro-inflammatory cytokines IL-1β and TNF-α ($P<0.05$) (Fig. 5a, b). The expression of molecules such as IL-6, IL-1RA, IL-10, VEGF-A, RANTES, and MIP1-α, and the MMP9/TIMP1 ratio were also not affected by the addition of LPS (Figs. 5 and 6). High glucose conditions were shown to increase the levels of pro-inflammatory cytokines TNF-α, IL-6 and anti-inflammatory IL-1RA. Under the same conditions, the secretion of chemokines RANTES, and MIP1-α levels were significantly decreased, while IL-1β, IL-10, VEGF-A, and MMP9 levels were not affected ($P<0.05$) (Figs. 5 and 6). High glucose media supplemented with LPS in the HGLPS group significantly increased pro-inflammatory cytokines IL-1β, TNF-α, IL-6 and anti-inflammatory molecules IL-1RA, IL-10, and VEGF-A. The same conditions significantly decreased the production of MMP9 but the levels of MIP1-α and RANTEs were not affected ($P<0.05$) (Figs. 5 and 6).

Macrophages-fibroblasts juxtacrine co-culture

When both macrophages and fibroblasts were mixed, the levels of IL-1β, TNF-α, IL-8, MCP-1, RANTES, MIP1-α and MIP1-β were not affected overall in any of the groups (Figs. 5 and 6). LPS treatment of the cells

under the normal glucose conditions, did not affect the levels of the molecules IL-6, IL-1RA, or VEGF-A rather it increased the levels of TGF-β, IL-10 and MMP9 (Figs. 5 and 6). High glucose media conditions significantly increased the anti-inflammatory cytokine TGF-β, decreased IL-1RA amounts, and the levels of IL-6, IL-10, VEGF-A, and MMP9 were not changed with respect to the baseline ($P<0.05$) (Figs. 5 and 6). High glucose and LPS combination media increased IL-1RA, TGF-β and decreased VEGF-A and MMP9 significantly ($P<0.05$) (Figs. 5 and 6). Although IL-6 and IL-10 did not differ from those at the baseline (NG), but their levels were significantly lower compared to LPS-infected group in normal glucose media i.e., NGLPS ($P<0.05$) (Fig. 5c, e).

Differential cytoskeletal element expression in fibroblasts

Vimentin

Fibroblasts in all the culture settings for all the groups expressed vimentin differentially. Macrophages monoculture was stained for vimentin as a control for juxtacrine culture setting. Macrophages were shown to express negligible amounts of vimentin. Vimentin expression was significantly lower in the HGLPS groups for all the monoculture and co-culture settings except for the paracrine culture for which it was not significantly different ($P<0.05$) (Fig. 7). In the juxtacrine set of the cells, addition of LPS in the normal glucose media significantly reduced the vimentin expression ($P<0.05$) (Fig. 7d).

Actin

Actin was differentially expressed in fibroblasts treated with different media conditions in all the monoculture and co-culture settings. Fibroblasts monoculture and juxtacrine co-culture with macrophages showed lower expression of actin under high glucose conditions both with and without LPS (Fig. 8a, d). Fibroblasts treated with macrophage conditioned media did not show any significant differences in the actin expression among all the groups. On the contrary, fibroblasts cultured in a continuous paracrine setting with macrophages presented reduced expression of actin under both high glucose and LPS, individually as well as in combination (Fig. 8b, c).

Discussion

Diabetic wounds with their prominent and prolonged inflammatory phase driven by M1 macrophages, face a significant challenge in transitioning towards the M2-like phenotypes for the repair process. This transition may not occur as expected in chronic wounds, and the influence of the microenvironment at the injured site on macrophage phenotypic plasticity is crucial. In this case, various factors including high glucose levels, bacterial infection, and AGEs, contribute to altered macrophage phenotypes. High glucose levels, a key factor in altered macrophage phenotypes, significantly reduces macrophage phagocytic activity, hindering infection clearance and nitric oxide production. In diabetic individuals, macrophages display hyperresponsiveness to inflammatory stimuli, which contributes to the prolonged inflammatory phase within the wound setting[42].

CD68, a pan macrophage marker indicates the presence of macrophages (neither M1 nor M2 polarized). Classically activated macrophages specifically express CD80 and STAT1, while CD206, STAT6, and STAT3 are specific markers of the M2 phenotype[43]. STAT6 is expressed when polarization is induced by IL-4 or IL-13, indicating the M2a subtype, whereas STAT3 is expressed when polarization is induced by IL-10 and IL-6, indicating the M2c subtype. Both the subtypes are involved in the tissue re-modeling phase of the wound healing[43]. A higher STAT1 expression induced by high glucose and AGE media supplemented with and without LPS indicates macrophages activation more towards a pro-inflammatory state under a hyperglycemic environment[44]. Moreover, hyperglycemia combined with and without LPS, reduced the expression of STAT3 and STAT6 indicating the M2 < M1 state of macrophages. This was further supported by the increase in CD80 expression, while CD206 was not expressed in all the groups.

Treatment of macrophages with high glucose and AGEs or LPS for 24 h lead to the production of chemokines (IL-8, MCP-1, and RANTES), and proteases (MMP9) and inhibit the production of IL-1RA (Fig. 9). LPS-mediated IL-1β further signals the macrophages in an autocrine manner to produce TNF-α and IL-6. LPS-induction alone also promoted the production of MIP chemokines MIP-1α and MIP-1β. The combination of high glucose, AGEs and LPS further enhanced the secretion of MIP-1β. High glucose (with AGEs) inhibited the anti-inflammatory molecule IL-10. An increase in the chemokines production and higher expression of M1 markers indicate that under an LPS-infected and/or hyperglycemic environment, macrophages are recruited to the wound site undergo increased polarization towards an M1 phenotype and could further recruit additional macrophages that will also be polarized to an inflammatory state. These findings are supported by evidence from in vivo studies reported in the literature. Chronic diabetic wounds are marked by low levels of chemokines (MCP-1 and RANTES) at the early phase of wound healing that delay the macrophage homing; however, at later stages these levels are extremely high indicating delayed and prolonged inflammation[45].

Stimulation of fibroblasts alone by LPS or high glucose (with AGEs) individually did not change the levels of TNF-α and IL-6, which might be because IL1-β was not secreted excluding the possibility of its autocrine effect (Fig. 9). IL-8 production was significantly higher ($P<0.05$) in the presence of high glucose (with AGEs), similar to findings in the literature in which epidermal cells (keratinocytes) led to a higher oxidative stress[46]. Interestingly, high glucose concentrations induced the secretion of VEGF-A and TGF-β by fibroblasts alone. TGF-β is constitutively produced by cells, and its high levels have been observed in early phases of wound healing as well, during which it acts as a chemotactic agent to recruit immune cells to the wound site[47]. Chemokines RANTES and MCP-1 production was significantly mediated by high glucose (with AGEs) and LPS alone. However, MCP-1 production was inhibited in the presence of the combination of high glucose, AGEs and LPS indicating the delayed infiltration of immune cells by the host cells. Previous studies have also reported lower MCP-1 levels in diabetic wounds[48].

LPS exposure has been identified as a critical initiating factor in wound healing in a dose dependent manner, with dermal fibroblasts playing an essential role in this process. The enhancement of cellular migration of dermal

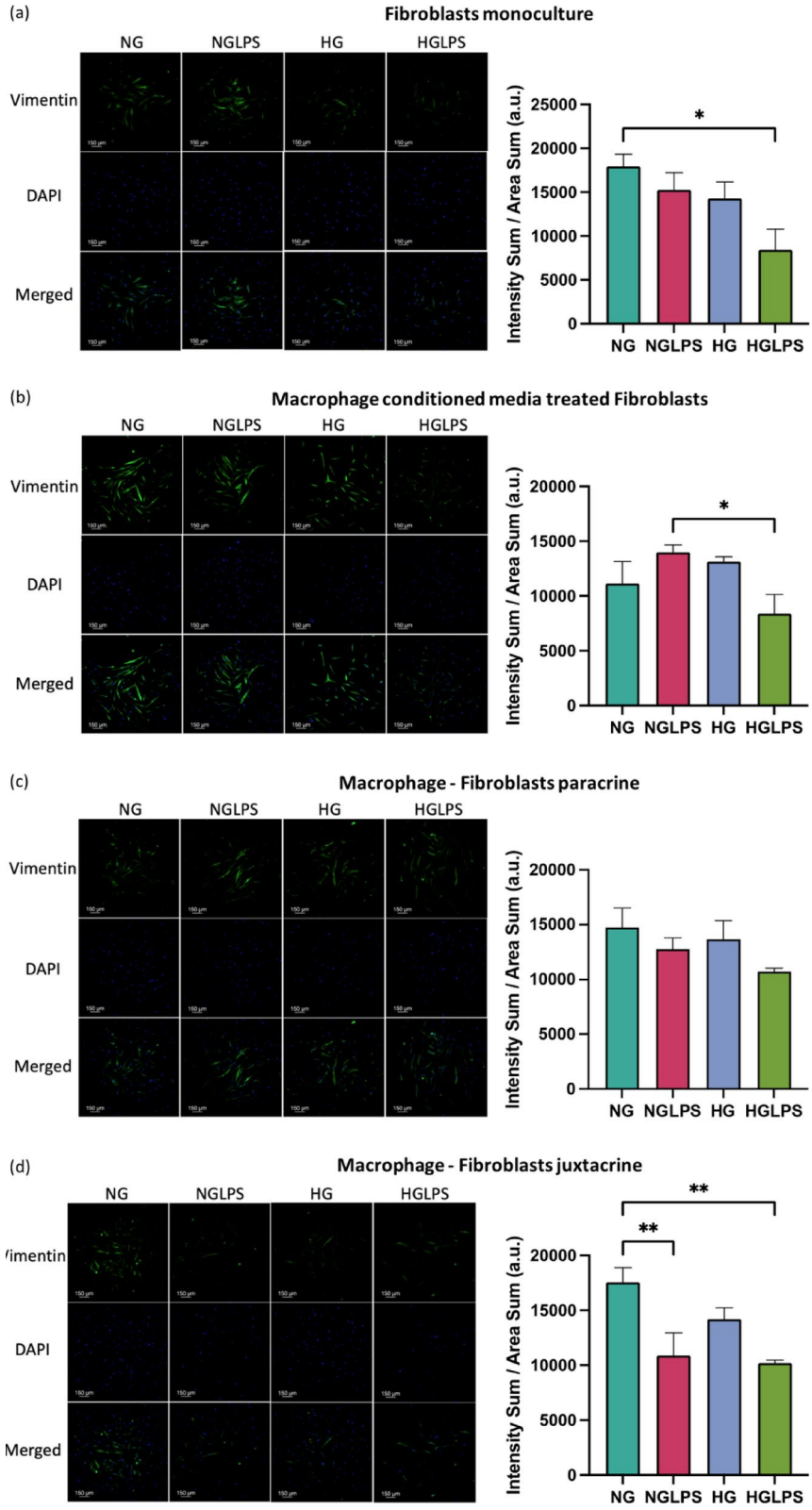

Fig. 7. Vimentin expression in fibroblasts under different monoculture and co-culture conditions.

fibroblasts alone post-LPS infection at a concentration of 1 μg/mL in normal glucose media may be mediated by stathmin and microtubule depolymerization via the p38/MAPK pathway[49]. Additionally, research has shown that p38 and ERK (extracellular signal-regulated) collectively regulate the wound healing process. Growth factors activate p38, which promotes epithelial migration, while ERK1/2 activation stimulates cell proliferation[50].

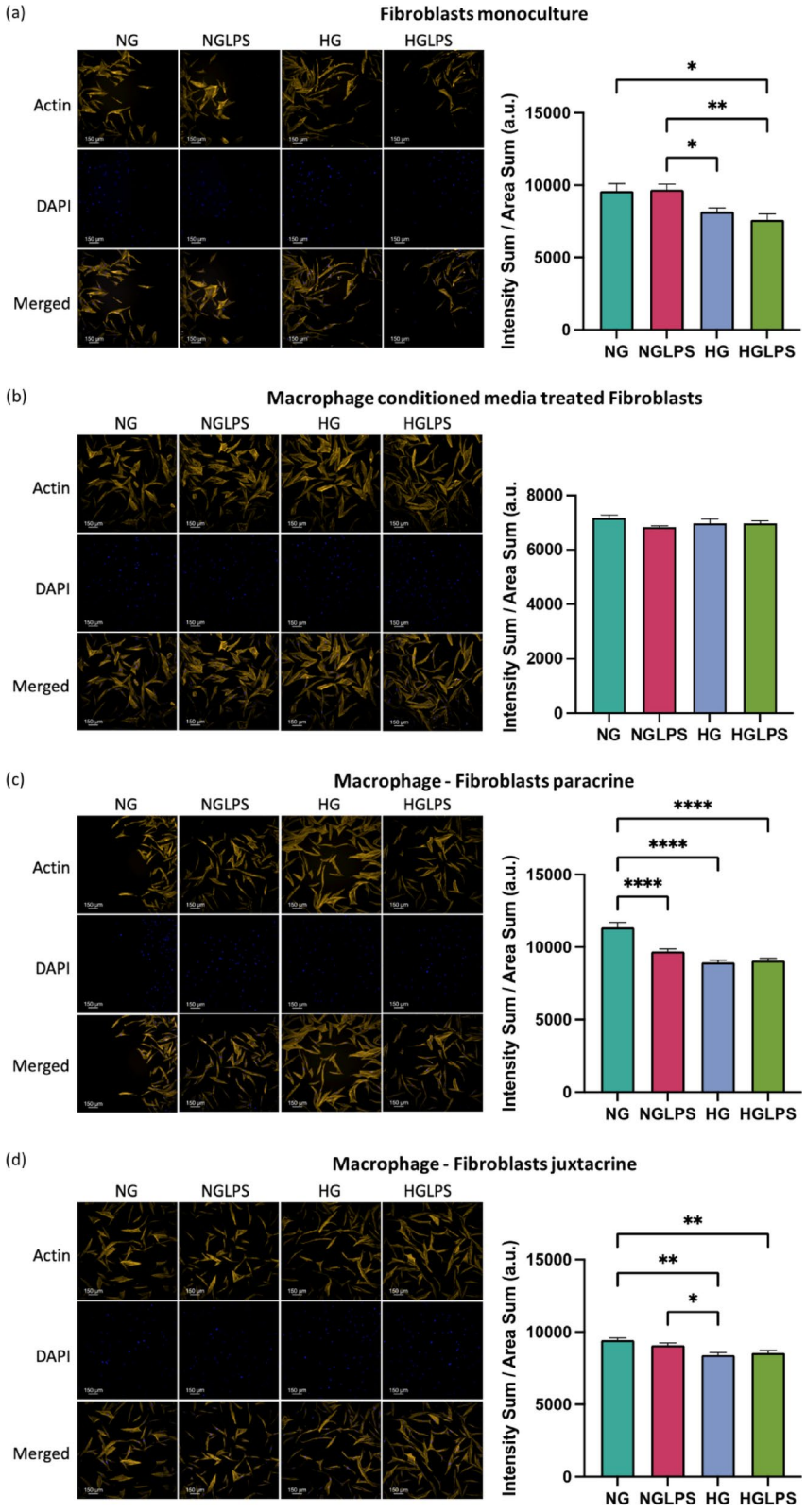

Fig. 8. Actin expression in fibroblasts under different monoculture and co-culture conditions.

Delayed fibroblasts migration due to a hyperglycemic environment indicated a delayed wound healing process in diabetic wounds. A high glucose concentration of 25mM can induce oxidative damage and impair fibroblasts' migration and proliferation[51]. Protein glycation and the formation of AGEs via non-enzymatic reactions play an essential role in the pathogenesis of diabetic complications. The accumulation of AGEs has also been associated

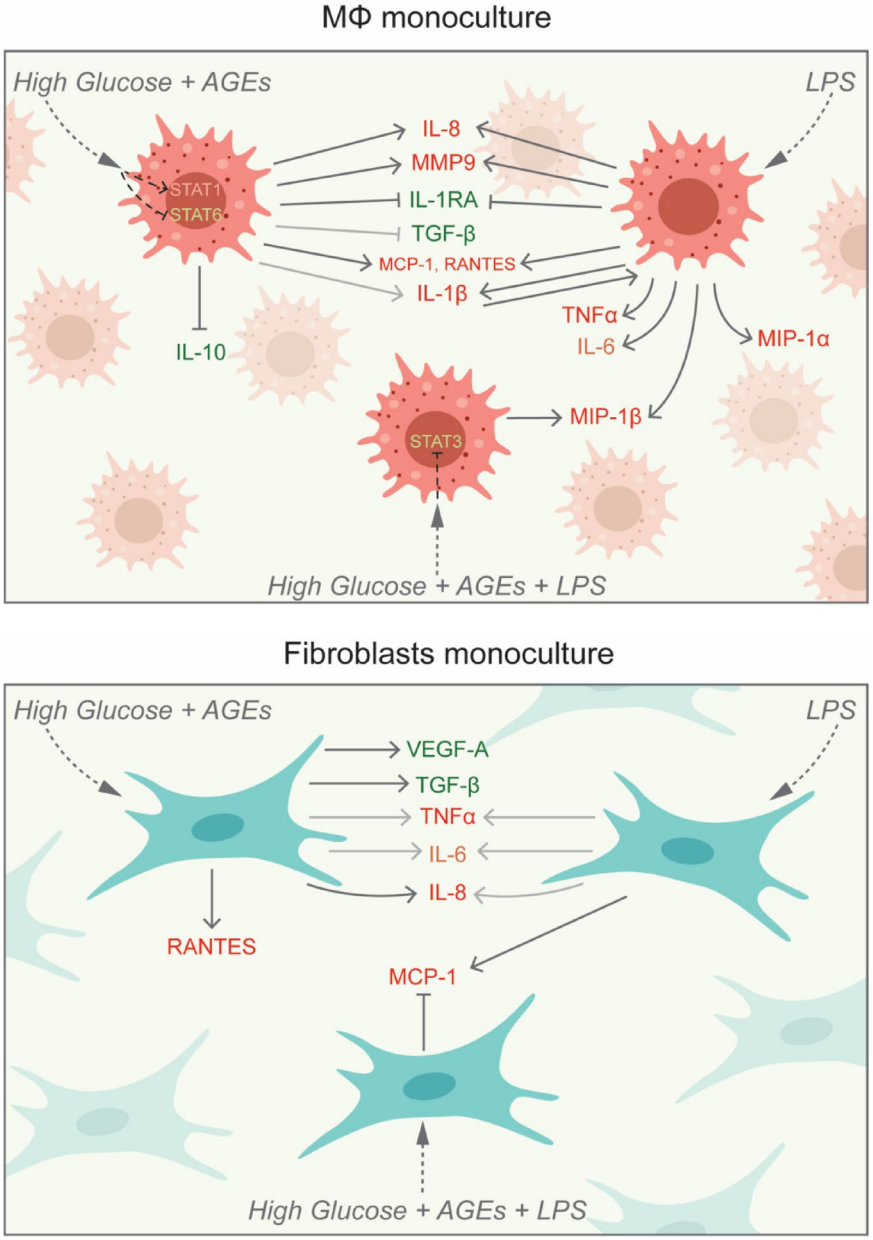

Fig. 9. Schematic showing autocrine signaling in macrophages and fibroblasts monocultures.

with enhanced apoptosis in fibroblasts through the activation of NLRP3 inflammasome via the ROS signaling pathway[52]. AGE activation of RAGE in fibroblasts can lower the contractility and turnover ability[53]. When bacterial LPS was added to a hyperglycemic environment, the overall migration of fibroblasts was worsened which was also evidenced by the lower actin expression in similar conditions. Cell's ability to respond to LPS as seen in normal glucose media is lost in high glucose media, making this combination even more deleterious. Vimentin, an intermediate filament protein, is expressed in mesenchymal cells and widely used as a marker for epithelial-to-mesenchymal transitions (EMT)[54]. Vimentin has also been shown to be involved in wound healing. Lower vimentin expression induced by hyperglycemia with and without LPS underscores the lower migratory potential of the cells under those conditions. Similar findings have been reported in human primary chronic wound-derived diabetic wounds fibroblasts[55]. Besides that, the role of vimentin in coordinating fibroblasts' proliferation and keratinocyte differentiation via the TGF-β-Slug signaling pathway has been established[56].

Paracrine interplay between macrophages and fibroblasts revealed that the secretion of cytokine triad IL-1β, TNF-α, and IL-6 was mediated by LPS, high glucose (with AGEs) and was more significantly affected by the combination of high glucose (with AGEs) and LPS (Fig. 10). Higher IL-1β secreted by macrophages could possibly have autocrine effects to produce more IL-1β and simultaneously induce the neighbouring fibroblasts to produce IL-1β, TNF-α, and IL-6. IL-6 production in this scenario was significantly mediated by high glucose (with AGEs) compared to LPS. Both high glucose (with AGEs) and LPS mediate MMP9 production by in paracrine signaling among fibroblasts and macrophages. The anti-inflammatory molecules VEGF-A and IL-

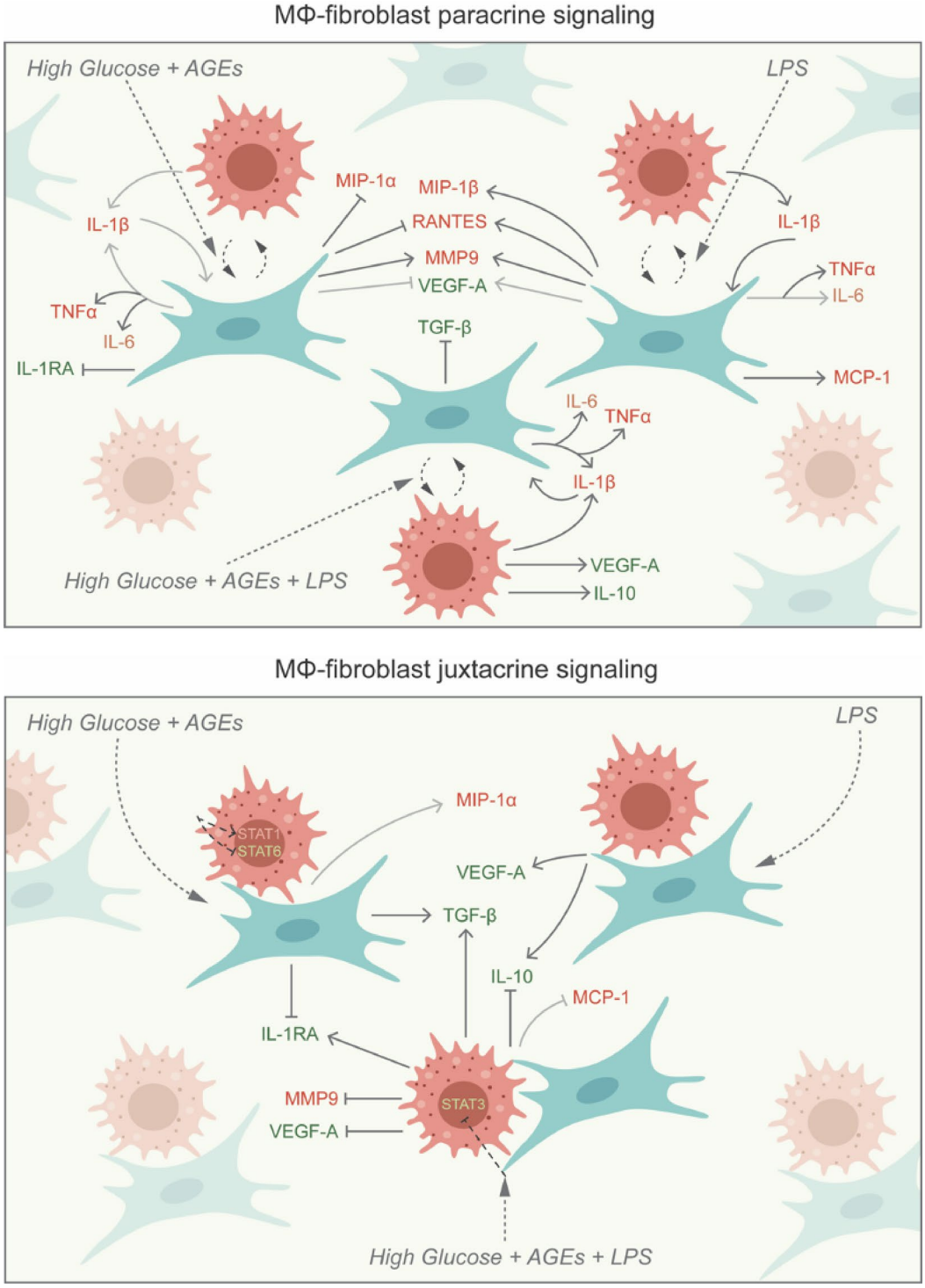

Fig. 10. Schematic showing paracrine and juxtacrine signaling in macrophage and fibroblast co-cultures.

1RA were inhibited by high glucose (with AGEs) while TGF-β was inhibited by the combination of high glucose (with AGEs) and LPS. Chemokines MCP-1, RANTES, and MIP-1β were induced by LPS treatment. However, RANTES secretion was inhibited by hyperglycemic presence as evidenced in the literature[57].

Cell-cell contact-specific signaling between macrophages and dermal fibroblasts represented juxtacrine crosstalk between the two cell types (Fig. 10). VEGF-A and IL-10 secretion was strongly mediated by LPS induction, whereas IL-10 secretion was inhibited by the combination of high glucose (with AGEs) and LPS during intercellular contact. Cell-cell contact decreased the levels of pro-inflammatory IL-6 and MMP9. It increased anti-inflammatory IL1-RA and TGF-β under an LPS-infected hyperglycemic environment highlighting the importance of direct contact between macrophages and fibroblasts for promoting healing.

In contrast, the reduced levels of anti-inflammatory molecules IL-10 and VEGF-A under similar conditions contradict the previous findings. MIP1-α secretion was increased in the presence of high glucose (with AGEs), although the difference was not significant. However, with the combination of high glucose (with AGEs) and LPS, MCP-1 secretion was inhibited but not significant, indicating delayed macrophage homing under hyperglycemia and bacterial infection. When compared to the dynamic paracrine interplay the juxtacrine setting having intercellular contact showed lower pro-inflammatory cytokines (IL-1β, TNF- α, and IL-6) and higher anti-inflammatory molecules (IL-1RA, TGF- β, and VEGF-A). This could be due to the macrophage polarizing more towards M2 phenotype which was also demonstrated by the higher expression of CD206 by these macrophages in the juxtacrine setting while CD206 was not expressed at all in the paracrine model (Fig. S1). Thus, establishing the 'macrophages-fibroblasts (immune-stromal) synapse' is important for ensuring wound healing homeostasis[58]. These findings were in line with the cellular migration analysis that showed equivalent levels of migration rate among different groups in the juxtacrine setting compared to the delayed migration rate induced by hyperglycemia in the paracrine setting. Hyperglycemia also reduced the expression of cytoskeletal proteins (vimentin and actin) in both paracrine and juxtacrine settings; however, the reduction was highly significant in paracrine crosstalk model. When fibroblasts were co-cultured with macrophages in either paracrine or juxtacrine settings, molecules secreted from macrophages depending on their polarization state can alter the migration of fibroblasts. When treated with high glucose and LPS, macrophages tend to polarize to a pro-inflammatory state secreting higher levels of pro-inflammatory molecules and high levels of proteases leading to delayed migration via paracrine signaling. Moreover, cell-cell contact regulates the pro-inflammatory molecules to a certain extent promoting wound healing.

Although this research study analyzes the dysfunctional crosstalk between macrophages and fibroblasts under hyperglycemic and LPS-infected conditions, it is important to recognize its limitations. A more in-depth investigation into the heterogeneity of dermal fibroblasts, particularly their activation into myofibroblast phenotypes, beyond migration and cytokine secretion, could improve our understanding of healthy wound healing process. Future studies should concentrate on the various subtypes of fibroblast, especially the transition from fibroblast-to-myofibroblast, and their impact on ECM remodeling using complex 3D wound healing models.

Furthermore, while we concentrated on key cellular signaling pathways, exploring molecular signaling cascades in macrophages and fibroblasts—such as the NF-κB, JAK-STAT, and MAPK pathways—could deepen our understanding of the underlying mechanisms. Furthermore, the lack of therapeutic testing limits the translational impact of this research. Investigating immunomodulatory interventions, such as cytokine blockers and anti-inflammatory bioactives, may offer valuable insights into the immune-stromal balance in diabetic wounds. Acknowledging these limitations, the current study establishes a foundation for future research aimed at developing diabetic wound models and therapeutic strategies that target macrophage-fibroblast interactions to enhance wound healing.

Conclusion

In a diabetic wound environment characterized by LPS and hyperglycemia, deficient chemokines (MCP-1, MIP1-α, and MIP-β) production by fibroblasts results in a delayed macrophage recruitment. This further delays the functional interplay of macrophages and fibroblasts in recovering the healing. These macrophages, polarized towards a pro-inflammatory state as evidenced by elevated CD80 and STAT1 expression, contribute to dysfunctional paracrine and juxtacrine interactions, initiating a pro-inflammatory cascade via high proteases (MMP9), pro-inflammatory (IL-1β, TNF-α, and IL-6), and low anti-inflammatory cytokines (IL-10, VEGF-A, and TGF-β), that impedes fibroblast migration, possibly through the inhibition of cytoskeletal proteins (vimentin and actin) (Fig. 11). Paracrine interaction governs the chronicity of the wound, producing a more pro-inflammatory milieu. Juxtacrine interaction between macrophages and fibroblasts gives rise to an 'immune-stromal synapse' that regulates the inflammation under hyperglycemia. Hence, timely recruitment of macrophages and M2 polarization are necessary for orchestrating healthy healing in diabetic wounds. These findings emphasize the necessity of immunomodulatory therapies for diabetic ulcers to shift the macrophages towards an alternatively activated state in which they are positive for CD206 expression and produce more anti-inflammatory molecules (IL-1RA, TGF-β, and VEGF-A). These findings also support the importance of exogenous cell-delivery therapeutic strategies, which have been demonstrated to enhance healing in diabetic wounds in animal models[58].

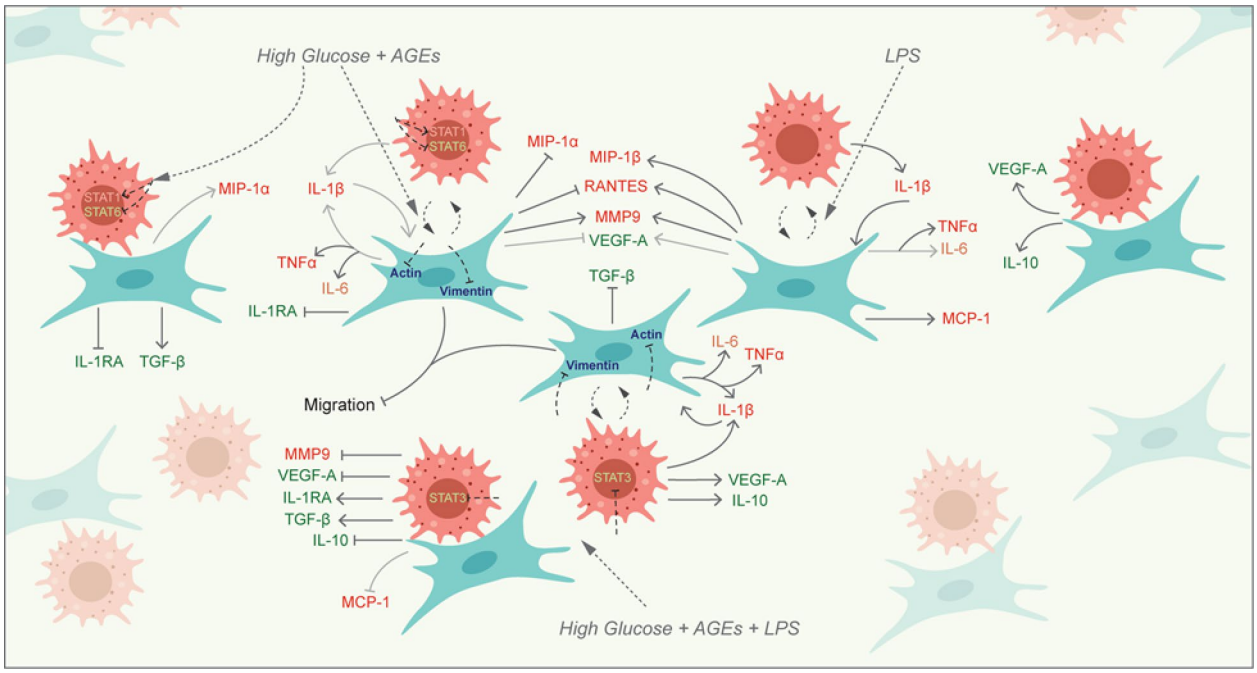

Fig. 11. Schematic showing the dysfunctional crosstalk between macrophages and fibroblasts under LPS-infected and hyperglycemic environment.

Data availability

All data generated or analysed during this study are included in this published article (and its Supplementary Information files).

Received: 21 October 2024; Accepted: 29 April 2025
Published online: 18 May 2025

References

1. Kaul, K., Tarr, J. M., Ahmad, S. I., Kohner, E. M. & Chibber, R. Introduction to diabetes mellitus. *Diabetes: Old Disease New. Insight* **771**, 1–11 (2013).
2. Sun, H. et al. IDF diabetes atlas: global, regional and country-level diabetes prevalence estimates for 2021 and projections for 2045. *Diabetes Res. Clin. Pract.* **183**, 109119 (2022).
3. Association, A. D. Diagnosis and classification of diabetes mellitus. *Diabetes Care.* **37**, S81–S90 (2014).
4. Sorber, R. & Abularrage, C. J. in *Seminars in Vascular Surgery*. 47–53 (2021)(Elsevier).
5. Lepäntalo, M. et al. Chapter V: diabetic foot. *Eur. J. Vasc. Endovasc. Surg.* **42**, S60–S74 (2011).
6. Zhang, P. et al. Global epidemiology of diabetic foot ulceration: a systematic review and meta-analysis. *Ann. Med.* **49**, 106–116 (2017).
7. Walsh, J., Hoffstad, O., Sullivan, M. & Margolis, D. Association of diabetic foot ulcer and death in a population-based cohort from the united Kingdom. *Diabet. Med.* **33**, 1493–1498 (2016).
8. Lemieux, I. *Vol. 12 1974* (MDPI, 2020).
9. Patel, S., Srivastava, S., Singh, M. R. & Singh, D. Mechanistic insight into diabetic wounds: pathogenesis, molecular targets and treatment strategies to Pace wound healing. *Biomed. Pharmacother.* **112**, 108615. https://doi.org/10.1016/j.biopha.2019.108615 (2019).
10. Thomas, D., O'neill, I., Harding, K. & Shepherd, J. Cutaneous wound healing: a current perspective. *J. Oral Maxillofac. Surg.* **53**, 442–447 (1995).
11. Stunova, A. & Vistejnova, L. Dermal fibroblasts—A heterogeneous population with regulatory function in wound healing. *Cytokine Growth Factor Rev.* **39**, 137–150 (2018).
12. Hackam, D. J. & Ford, H. R. Cellular, biochemical, and clinical aspects of wound healing. *Surg. Infect.* **3**, s23–s35 (2002).
13. Park, J. E. & Barbul, A. Understanding the role of immune regulation in wound healing. *Am. J. Surg.* **187**, S11–S16 (2004).
14. Snyder, R. J. et al. Macrophages: a review of their role in wound healing and their therapeutic use. *Wound Repair. Regeneration*. **24**, 613–629 (2016).
15. Tracy, L. E., Minasian, R. A. & Caterson, E. Extracellular matrix and dermal fibroblast function in the healing wound. *Adv. Wound Care.* **5**, 119–136 (2016).
16. Xue, M., Zhao, R., March, L. & Jackson, C. Dermal fibroblast heterogeneity and its contribution to the skin repair and regeneration. *Adv. Wound Care.* **11**, 87–107 (2022).
17. Wynn, T. A. & Vannella, K. M. Macrophages in tissue repair, regeneration, and fibrosis. *Immunity* **44**, 450–462 (2016).
18. Shook, B. A. et al. Myofibroblast proliferation and heterogeneity are supported by macrophages during skin repair. *Science* **362**, eaar2971 (2018).
19. Willenborg, S. & Eming, S. A. Cellular networks in wound healing. *Science* **362**, 891–892 (2018).
20. Ploeger, D. T. et al. Cell plasticity in wound healing: paracrine factors of M1/M2 polarized macrophages influence the phenotypical state of dermal fibroblasts. *Cell. Communication Signal.* **11**, 1–17 (2013).
21. Buechler, M. B., Fu, W. & Turley, S. J. Fibroblast-macrophage reciprocal interactions in health, fibrosis, and cancer. *Immunity* **54**, 903–915 (2021).

22. Zhu, Z., Ding, J., Ma, Z., Iwashina, T. & Tredget, E. E. Alternatively activated macrophages derived from THP-1 cells promote the fibrogenic activities of human dermal fibroblasts. *Wound Repair. Regeneration*. **25**, 377–388 (2017).
23. Murray, P. J. & Wynn, T. A. Protective and pathogenic functions of macrophage subsets. *Nat. Rev. Immunol.* **11**, 723–737 (2011).
24. Zhang, S. M. et al. M2-polarized macrophages mediate wound healing by regulating connective tissue growth factor via AKT, ERK1/2, and STAT3 signaling pathways. *Mol. Biol. Rep.* **48**, 6443–6456 (2021).
25. Kim, S. W. et al. Delivery of a spheroids-incorporated human dermal fibroblast sheet increases angiogenesis and M2 polarization for wound healing. *Biomaterials* **275**, 120954 (2021).
26. Davis, F. M., Kimball, A., Boniakowski, A. & Gallagher, K. Dysfunctional wound healing in diabetic foot ulcers: new crossroads. *Curr. Diab Rep.* **18**, 2. https://doi.org/10.1007/s11892-018-0970-z (2018).
27. Brem, H. & Tomic-Canic, M. Cellular and molecular basis of wound healing in diabetes. *J. Clin. Invest.* **117**, 1219–1222. https://doi.org/10.1172/JCI32169 (2007).
28. Armstrong, D. G., Boulton, A. J. & Bus, S. A. Diabetic foot ulcers and their recurrence. *N. Engl. J. Med.* **376**, 2367–2375 (2017).
29. Lerman, O. Z., Galiano, R. D., Armour, M., Levine, J. P. & Gurtner, G. C. Cellular dysfunction in the diabetic fibroblast: impairment in migration, vascular endothelial growth factor production, and response to hypoxia. *Am. J. Pathol.* **162**, 303–312 (2003).
30. Theocharidis, G. et al. Single cell transcriptomic landscape of diabetic foot ulcers. *Nat. Commun.* **13**, 181 (2022).
31. Shapouri-Moghaddam, A. et al. Macrophage plasticity, polarization, and function in health and disease. *J. Cell. Physiol.* **233**, 6425–6440 (2018).
32. del Mar Cendra, M. & Torrents, E. Pseudomonas aeruginosa biofilms and their partners in crime. *Biotechnol. Adv.* **49**, 107734 (2021).
33. Westby, M. J., Norman, G., Watson, R. E., Cullum, N. A. & Dumville, J. C. Protease activity as a prognostic factor for wound healing in complex wounds. *Wound Repair. Regeneration*. **28**, 631–644 (2020).
34. Tchanque-Fossuo, C. N., Dahle, S. E., Buchman, S. R. & Isseroff, R. R. Deferoxamine: potential novel topical therapeutic for chronic wounds. *Br. J. Dermatol.* **176**, 1056–1059. https://doi.org/10.1111/bjd.14956 (2017).
35. Daneshpour, H. & Youk, H. Modeling cell–cell communication for immune systems across space and time. *Curr. Opin. Syst. Biology*. **18**, 44–52 (2019).
36. Yang, B. A., Westerhof, T. M., Sabin, K., Merajver, S. D. & Aguilar, C. A. Engineered tools to study intercellular communication. *Adv. Sci.* **8**, 2002825 (2021).
37. Das, A., Ganesh, K., Khanna, S., Sen, C. K. & Roy, S. Engulfment of apoptotic cells by macrophages: a role of microRNA-21 in the resolution of wound inflammation. *J. Immunol.* **192**, 1120–1129 (2014).
38. Yu, J., Nam, D. & Park, K. S. Substance P enhances cellular migration and inhibits senescence in human dermal fibroblasts under hyperglycemic conditions. *Biochem. Biophys. Res. Commun.* **522**, 917–923. https://doi.org/10.1016/j.bbrc.2019.11.172 (2020).
39. Ono, Y. et al. Increased serum levels of advanced glycation end-products and diabetic complications. *Diabetes Res. Clin. Pract.* **41**, 131–137 (1998).
40. Takahashi, H. K. et al. Advanced glycation end products subspecies-selectively induce adhesion molecule expression and cytokine production in human peripheral blood mononuclear cells. *J. Pharmacol. Exp. Ther.* **330**, 89–98 (2009).
41. Suarez-Arnedo, A. et al. An image J plugin for the high throughput image analysis of in vitro scratch wound healing assays. *PloS One*. **15**, e0232565 (2020).
42. Aitcheson, S. M., Frentiu, F. D., Hurn, S. E. & Edwards, K. Murray, R. Z. Skin wound healing: normal macrophage function and macrophage dysfunction in diabetic wounds. *Molecules* **26**, 4917 (2021).
43. Chen, S. et al. Macrophages in immunoregulation and therapeutics. *Signal. Transduct. Target. Therapy*. **8**, 207 (2023).
44. Huang, S. M. et al. High glucose environment induces M1 macrophage polarization that impairs keratinocyte migration via TNF-α: an important mechanism to delay the diabetic wound healing. *J. Dermatol. Sci.* **96**, 159–167 (2019).
45. Wetzler, C., Kämpfer, H., Stallmeyer, B., Pfeilschifter, J. & Frank, S. Large and sustained induction of chemokines during impaired wound healing in the genetically diabetic mouse: prolonged persistence of neutrophils and macrophages during the late phase of repair. *J. Invest. Dermatology*. **115**, 245–253 (2000).
46. Lan, C. C. E., Wu, C. S., Huang, S. M., Wu, I. H. & Chen, G. S. High-glucose environment enhanced oxidative stress and increased interleukin-8 secretion from keratinocytes: new insights into impaired diabetic wound healing. *Diabetes* **62**, 2530–2538 (2013).
47. Werner, S. & Grose, R. Regulation of wound healing by growth factors and cytokines. *Physiol. Rev.* **83**, 835–870 (2003).
48. DeClue, C. E. & Shornick, L. P. The cytokine milieu of diabetic wounds. *Diabetes Manage.* **5**, 525–537 (2015).
49. Cen, R. et al. Dermal fibroblast migration and proliferation upon wounding or lipopolysaccharide exposure is mediated by stathmin. *Front. Pharmacol.* **12**, 781282 (2022).
50. Sharma, G. D., He, J. & Bazan, H. E. p38 and ERK1/2 coordinate cellular migration and proliferation in epithelial wound healing: evidence of cross-talk activation between MAP kinase cascades. *J. Biol. Chem.* **278**, 21989–21997 (2003).
51. Buranasin, P. et al. High glucose-induced oxidative stress impairs proliferation and migration of human gingival fibroblasts. *PLoS One*. **13**, e0201855. https://doi.org/10.1371/journal.pone.0201855 (2018).
52. Dai, J., Chen, H. & Chai, Y. Advanced glycation end products (AGEs) induce apoptosis of fibroblasts by activation of NLRP3 inflammasome via reactive oxygen species (ROS) signaling pathway. *Med. Sci. Monitor: Int. Med. J. Experimental Clin. Res.* **25**, 7499 (2019).
53. Van Putte, L., De Schrijver, S. & Moortgat, P. The effects of advanced glycation end products (AGEs) on dermal wound healing and Scar formation: a systematic review. *Scars Burns Healing*. **2**, 2059513116676828 (2016).
54. Ostrowska-Podhorodecka, Z. & McCulloch, C. A. Vimentin regulates the assembly and function of matrix adhesions. *Wound Repair. Regeneration*. **29**, 602–612 (2021).
55. Monika, P. et al. Human primary chronic wound derived fibroblasts demonstrate differential pattern in expression of fibroblast specific markers, cell cycle arrest and reduced proliferation. *Exp. Mol. Pathol.* **127**, 104803 (2022).
56. Cheng, F. et al. Vimentin coordinates fibroblast proliferation and keratinocyte differentiation in wound healing via TGF-β–Slug signaling. *Proc. Natl. Acad. Sci.* **113**, E4320–E4327 (2016).
57. Strang, H. et al. *In Wound Healing, Tissue Repair, and Regeneration in Diabetes*197–235 (Elsevier, 2020).
58. Hu, M. S. et al. Delivery of monocyte lineage cells in a biomimetic scaffold enhances tissue repair. *JCI Insight* **2**, 2 (2017).

Acknowledgements

The authors gratefully acknowledge the financial support from the Natural Sciences and Engineering Research Council of Canada (Discovery grant) (AK-RGPIN-2020-05844), the Canada Research Chair program (AK), and the Dr. Lloyd and Mrs. Kay Chapman Chairship.We would like to thank the Imaging Facility at the Hospital for Sick Children, Toronto for providing the microscopic and imaging facilities essential for this study. We also extend our gratitude to the SPARC Biocentre and Analytical Facility for Bioactive Molecules (AFBM) at The Hospital for Sick Children, Toronto for their support with the multiplex analysis services.

Author contributions

SS designed the research, performed the experiments, analyzed the data, interpreted the data, prepared the fig-

ures, and wrote the manuscript. AK designed the research, supervised the work, interpreted the data, and edited the manuscript. All the authors read and approved the final manuscript.

Declarations

Competing interests
The authors declare no competing interests.

Additional information
Supplementary Information The online version contains supplementary material available at https://doi.org/10.1038/s41598-025-00673-4.

Correspondence and requests for materials should be addressed to A.K.

Reprints and permissions information is available at www.nature.com/reprints.

Publisher's note Springer Nature remains neutral with regard to jurisdictional claims in published maps and institutional affiliations.